Biofilm microfacies in phosphoritic units of the Neoproterozoic Halkal Shale, Bhima basin, South India

Yogmaya Shukla[a,*], Mukund Sharma[a], Nora Noffke[b], Flavia Callefo[c]

[a] *Birbal Sahni Institute of Palaeosciences, 53 University Road, Lucknow 226007, India*
[b] *Old Dominion University, Ocean, Earth and Atmospheric Sciences, 329 Oceanography and Physics Building, Norfolk, VA 23529, USA*
[c] *Brazilian Synchrotron Light Laboratory (LNLS), Brazilian Centre for Research in Energy and Material (CNPEM), 13083-970 Campinas, Brazil*

ARTICLE INFO

ABSTRACT

The phosphatic bands of the Halkal Shale of the Neoproterozoic Bhima Basin, record an anoxic paleoenvironment, where only a few episodic depositional events introduced oxygen. In thin-sections, five distinct microfacies, caused by biofilms colonizing the ancient sea floor, can be distinguished. The microfacies document that low sedimentation rate allowed growth of biomass-rich laminae sets, whereas episodic influx of sand led to stacks of organic laminae alternating with fine sandy interlayers. Such depositional events may have also caused local rupture of biofilms and the release of small biofilm roll-ups and clasts. The ancient biofilms led to precipitation of phosphorous and iron-rich minerals and likely contributed to phosphorite formation. In modern equivalent environments, sea floor-colonizing biofilms include a high abundance of sulfide oxidizing and sulphate reducing bacteria.

1. Introduction

Fossil biofilms in marine paleoenvironments are common appearances (e.g., Schieber, 1986, 1989; Walsh and Lowe, 1999; Westall and Folk, 2003; Tice and Lowe, 2004, 2006; Tice, 2009; Noffke, 2000, 2010; Heubeck, 2009; Gamper et al., 2012). Occurrences in phosphorites have been documented by Banerjee (1971a,b), who described phosphatic stromatolites in the Paleoproterozoic rocks of Jhamarkotra region of Rajasthan, India. Hiatt et al. (2015) documented an example of fossil bacteria and biofilms associated with phosphogenesis from the Paleoproterozoic 1.85 Ga Michigamme Formation. Crosby et al. (2014) and Sallstedt et al. (2017) recorded microbial fossils in the Jhamarkotra stromatolites. Many others have documented examples in the Phanerozoic (e.g., Soudry and Champetier, 1983; Nathan et al., 1993; Lamboy, 1994; Arning et al., 2009). Some reports describe the microbial influence on the phosphogenic process, such as by cyanobacteria in Doushantuo phosphorites, China (She et al., 2013); and to sulphur bacteria in the 2 Ga Zaonega Formation, northwest Russia (Lepland et al., 2013). Such biofilms are diagenetically preserved by *in situ* replacement of the organic matter by minerals (Noffke, 2010).

The phosphorite accumulation during the Phanerozoic appears to be related to the primary productivity in the oceans (Filippelli and Delaney, 1994), however, the driving mechanism during the accumulation of phosphorites in the Precambrian remains unresolved (Nelson et al., 2010). It is known that the occurrence of phosphorites in Proterozoic is restricted to some periods of global biogeochemical changes (Papineau, 2010). The earliest phosphogenic event occurred during the Paleoproterozoic, that is linked to the oxygenation of the oceans and the atmosphere caused by the advent of oxygenic photosynthesis (Papineau, 2010).

Proterozoic phosphorites record worldwide changes such as: (1) the appearance of multicellular life, which affected benthic microbial colonization of the seafloor (Seilacher, 1999; Fedonkin, 2003; Dornbos et al., 2004; Dzik, 2007); (2) changes in ocean chemistry caused by the Neoproterozoic Oxygenation Event (NOE), great glacial events and the breakup of the Rodinia Supercontinent (Canfield et al., 2007; Och and Shields-Zhou, 2012); and (3) the Neoproterozoic/Cambrian phosphogenic episode, the Earth's second major phosphatic interval (Papineau, 2010; Pufahl, 2010; Papineau et al., 2013). Often, microbial substrates played a key role in the origin of phosphorites deposits (Caird et al., 2017). The Neoproterozoic-Cambrian time interval help understand the challenges faced by the benthic life forms due to advent and evolution of the multicellular life and the decline of precipitated stromatolites (Awramik, 1971, 1991; Riding, 2006); during this time period the mineral carbonate and phosphate played a crucial role in the process of biomineralization in the organisms. Our contribution aims to discuss the biogenicity of putative biofilms in the Neoproterozoic phosphatic lithologies of the Halkal Shale, Bhima Group, south India. The biofilms

---

* Corresponding author.
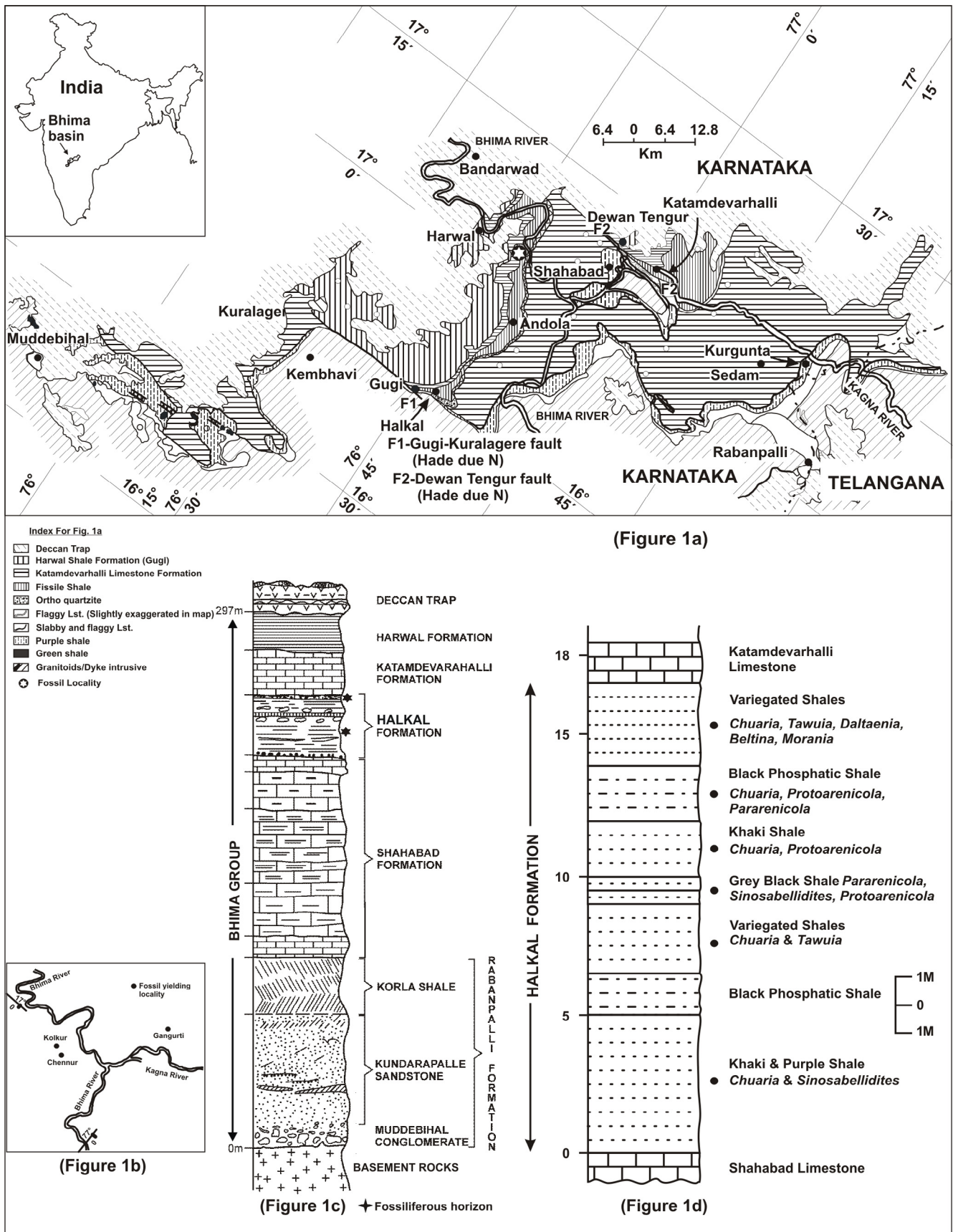 *E-mail address:* yogmayashukla@bsip.res.in (Y. Shukla).

Fig. 1. Geographical and geological map of the study area. (1a) Position of Bhima Basin on the map of India. (1b) Location of the sample sites in the Gulbarga district (not to scale). (1c) Lithostratigraphic section of the Bhima Group (after Jayaprakash, 2007). (1d) Stratigraphic section of the Halkal Shale, Bhima Group.

are described and an explanation about the possible microbial mechanism responsible for the deposition is offered. Outcrops of the Halkal Shale may represent a rare occurrence of significant dimensions for microbial phosphorites of the Neoproterozoic, never before documented from India.

2. Geology, age and depositional environment

2.1. Geology

The Bhima Group, occupying an area of ~5000 km², was deposited on the Archaean granite and greenstone terrain of the Dharwar Craton and overlain by the Upper Cretaceous-Paleocene Deccan Volcanic Province (Fig. 1). It is the smallest Proterozoic Basin in India and crops out in the Gulbarga district of Karnataka State and the Mehboobnagar and Rangareddy districts of Telangana State in south India. Geology and lithostratigraphy of the Bhima Group have been established over the last 150 years (Foote, 1876; Mahadevan, 1947; Janardhan Rao et al., 1975; Mishra et al., 1987; Kale et al., 1990; Kale and Peshwa, 1995; Jayaprakash, 2007). Various lithostratigraphic schemata were proposed for divisions of the rocks of the Bhima basin *viz.*, two fold subdivision, (Foote, 1876; Mishra et al., 1987); three fold sub-divisions *viz.*, Upper, Middle and Lower (Mahadevan, 1947); five-fold sub-division ascribed to two cycles of sedimentation (Janardhan Rao et al., 1975; Malur and Nagendra, 1994). On the basis of facies analysis of various litho-successions, a bipartite classification for the Bhima Group has been proposed and it was concluded that the clastic and carbonate facies rocks are the product of a single shallow marine transgression onto an epicontinental depression (Kale et al., 1990; Kale and Peshwa, 1995). Lithology includes largely unmetamorphosed sandstones, shales, and limestones, with limited occurrences of conglomerate (Mishra et al., 1987; Kale and Peshwa, 1995; Jayaprakash, 2007). Jayaprakash (2007) revised the classification of the Bhima Group and reiterated the existence of five formations namely the Rabanpalli Formation, the Shahabad Formation, the Halkal Formation, the Katamadevarhalli Formation, and the Harwal Formation aggregating to 297 m. Sood and Syamal Rao (1984) reported the presence of phosphorite in the Harwal Formation, north of Gogi and in the Korla Shale north of Darshanpur, where P_2O_5 ranges between 15% and 18%. Rocks of different formations of the Bhima Group are horizontal and exposed in low lying hillocks, at isolated places. They are seldom seen in natural contact (*i.e.,* overlying or underlying) thereby posing a concern for evolving a consensus on lithostratigraphic sub-division. In a very restricted area near Hotpet village (N 16°45′; E 76°47′), tectonically disturbed vertical to near-vertical beds of sandstone overlie the Halkal Formation. These beds are classified as the Hotpet Formation. Massive coarse-grained sandstone followed by flaggy limestones constitutes this formation. Well preserved mat structures have been noticed in the Halkal and the Hotpet formations (Shukla, 2011). Some Ediacaran fossils are recorded from Hotpet Formation (Sun and Sharma, 2016).

2.1.1. Halkal Formation

In the Bhima basin, phosphorite occurs in the form of thin beds in the Halkal Formation which is chiefly constituted of shale and siltstone. The contact of the Halkal Shale with the underlying Shahabad Limestone and the overlying Katamadevarhalli Formation is seen near the village Halkal (16°53′; 76°49′). The best exposure of the Halkal Shale is seen in Kolkur village (17°4′; 76°45′). In between the shales, phosphatic bands and nodules are seen in outcrops near Chennur (16°59′; 76°46′), Gangurthi (17°14′; 77°03′) (Fig. 2), Danduti (17°10′; 77°06′), Jewargi (17°00′; 76°46′) and Hagargundigi (17°09′; 76°44′). These shales are fissile and friable and greenish yellow to buff coloured. Das Sarma et al. (1992) reported the presence of phosphatic nodules in the Halkal Formation in the Kolkur village. In Gangurthi, centimeter-thick phosphorite bands are present at three levels in the Halkal Shales (Fig. 2) and designated as upper, middle, and lower bands. These bands
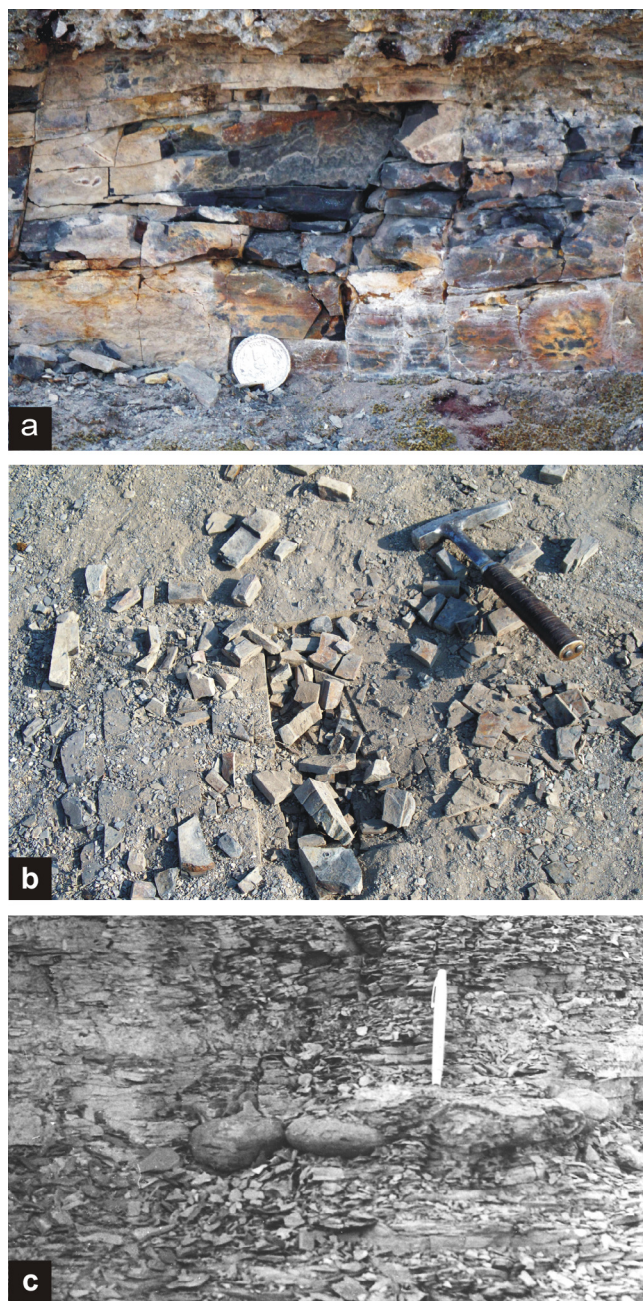

Fig. 2. Field exposures of phosphorite bands of the Halkal Shale seen near Gangurthi area. (a-b). Note bedded nature of phosphorite; (c) Phosphatic nodules seen near Chennur locality, these nodules occur parallel to the bedding planes.

of phosphorite are hard and dark brown to black in colour and are constituted of phosphatic laminae and phosphate particles set in a silt-size quartz matrix. Black and brown laminae are characteristic in the analyzed samples. The brown layers are composed of nearly homogenous phosphate ground mass with an organic network of fossil microbial filaments; the dark layers are phosphatic in nature with no discernible fossil occurrence. Kale and Peshwa's (1995) study show that none of the Bhima sediments (both carbonate and clastics) were deposited at a depth exceeding 10 m. The phosphorite bands are considered to have been deposited in a shallow, near-shore environment; the shale units possibly even in depths of less than five meters.

2.2. Age

On the basis of U-Pb and Sm-Nd Isotopic studies of the uraniferous brecciated limestone in the Gogi area, Pandey et al. (2008) suggested that the age of the Bhima basin is 1270 Ma. Comprehensive studies of limestone xenolith (purportedly part of the Shahabad Formation) by Dongre et al. (2008) and Chalapathi Rao et al. (2010) suggest Late Mesoproterozoic age (older than 1090 Ma) for the Bhima sediments. C and O isotopes proposed a post-Varanger depositional age for the Bhima sedimentary rocks (Kumar et al., 1999).

Microfossil assemblages recovered by several palynologists helped assign the age for the basin (Salujha et al., 1970; Srinivasa and Sambe Gowda, 1970; Venkatachala and Rawat, 1973; Viswanathiah et al., 1976). Sharma and Shukla (1996, 2012) reported various carbonaceous macrofossils and based on those fossils, assigned a Neoproterozoic age to the basin. Suresh and Sundara Raju (1983); Das Sarma et al. (1992); Sharma and Shukla (1996, 2012); and Maithy and Babu (1996) reported carbonaceous forms attributed to *Sinosabellidites huainanensis*, *Protoarenicola baiguashanensis*, *Pararenicola huaiyuanensis*, *Chuaria circularis* and *Tawuia dalensis* and assigned the Neoproterozoic age to the basin. The age of the Bhima sedimentary rocks is still under debate, but at present, a Neoproterozoic age is favored.

2.3. Depositional paleoenvironment

The Bhima basin is constituted of horizontal or nearly horizontally-layered sequences of unmetamorphosed and tectonically-low deformed sedimentary rocks. Chemogenic deposits of greater thickness with intercalated thin clastic deposits suggest a relatively stable depositional realm, whereas alternating clastic and chemogenic lithofacies, such as rudites followed by granular siliciclastic rocks, mud rocks and thick carbonate in distal shelf-facies and succeeded by another shale-carbonate-shale sequence, indicate a paleosetting of periodic depositional events (Mishra et al., 1987).

Sedimentation in the Bhima basin commenced with the deposition of a thin conglomerate/grit bed marking the Eparchaean unconformity. Pebbly character of the lowermost beds and preservation of a set of sedimentary structures, such as rill marks, ripple marks, and desiccation cracks (Akhtar, 1977), are suggestive of very shallow water conditions of the tidal flat environment. The other sedimentological studies indicate that the coarse clastics were deposited in the supratidal to intertidal zones, while the siltstone and shales were deposited in the intertidal to subtidal depositional zones of the shallow marine setting (Kale et al., 1990; Kale and Peshwa, 1995). In the Halkal Shales, the grey, khaki green, blackish buff colors of the lower beds are characteristic of euxinic to hypersaline environments, whereas, the pale pink to flesh red colors are attributed to agitated water circulation and exposure to the atmosphere which allowed the iron-oxides to attain ferric state (Jayaprakash, 2007). Mathur (1979) reported presence of glauconite in an outcrop of a flaggy, fine-grained sandstone and siltstone sequence near Udmeshwaran which belonged to the lower Bhima Formation (=Rabanapalli Shale named by Mathur, 1977). Presence of glauconite in sandstone also confirms a marine influence indicating that the lower Bhima beds were possibly deposited slowly under saline, weekly reducing shallow marine conditions (Mathur, 1977; Mudholkar and Kale, 1982; Jayaprakash, 2007). Hydrodynamically stable conditions in the basin resulted in the deposition of thick limestone beds above the shales. Alternating limestone and clastic facies towards the top are indicative of increasing hydrodynamic action in the basin. Geochemical studies suggest hydrodynamically calm closed-basin conditions for the Bhima basin such as those prevailing in a modern hypersaline environment (Sathyanarayan et al., 1987).

3. Material and methods

Microscopic facies are well preserved in the phosphatic units of the Halkal Formation. In order to study the facies, petrographic thin sections of the phosphatic bands were investigated under light microscope (Nikon Eclipse 80*i*). Raman spectroscopy analyses were carried out at Birbal Sahni Institute of Palaeosciences on a Renishaw 588v04 integrated Confocal Raman System and its library. For Raman analysis, standard uncovered petrographic thin sections were prepared that allowed optical and chemical maps to be superimposed. All the analyses were carried out by using a 514 nm laser, 2400 l/mm grating, and 20X objective lens. Focus mode was regular. Maps were acquired using the obtained Raman spectra. Because carbon and hematite both have major peaks in the 1320–1350 cm^{-1} region, the presence of organic carbon is confirmed using the 1600 cm^{-1} peak (Marshall et al., 2011; Noffke et al., 2013; Bower et al., 2016). Quantitative X-ray-diffraction measurements of the different bands of phosphorite samples were carried out on a Rigaku D/MAX 2400 X-ray diffractometer with a wide-angle goniometer at the Indian Institute of Technology, Bombay, Mumbai, India. Samples were ground using mortar and pestle and sieved to prepare homogeneous fine powder (1–50 μm) and placed in the diffractometer. The equipment was set on the following specification. X-Ray Anode: Cu – kα (λ = 1.54056 A); Scan Range: 5.0–60.0 (°2θ); Step Size: 0.02; Scan Speed: 3°/min; Voltage and current: 40 kV and 20 mA. The 2θ of each major reflection is measured and compared with analyses of standards. England Finder coordinates and slide numbers are provided for all the illustrated biofilm facies in thin sections which are deposited in the repository of the Birbal Sahni Institute of Palaeosciences, Lucknow, India under statement no. 1484.

4. Results
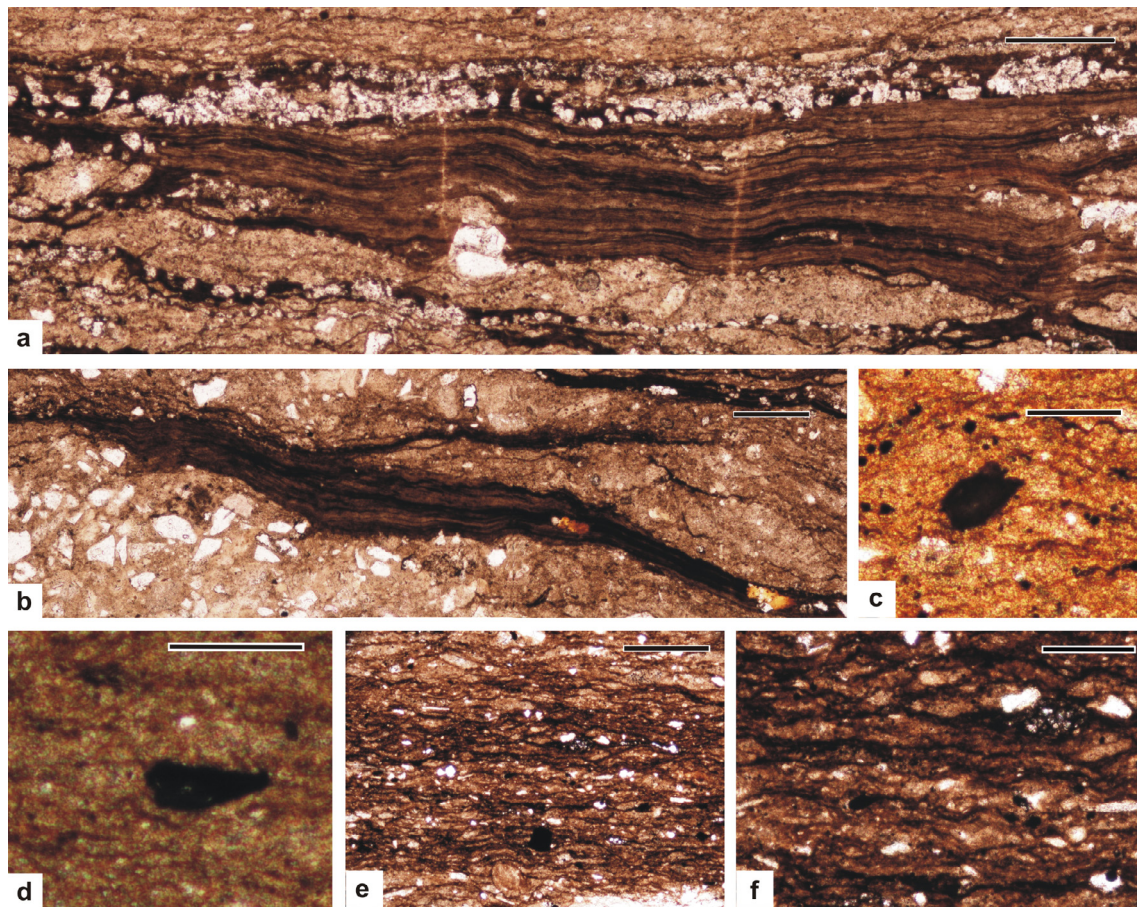
4.1. Biofilm microfacies

A succession of carbonaceous shale and siltstone of the Halkal Formation exposed near Gangurthi includes phosphatic bands. In thin-sections perpendicular to the bedding, the phosphorite bands display a great variety of microfacies. The microfacies are of μm to mm scales and characterized by brown-opaque microfacies resembling the net-work of a microbial mat composed of filamentous textures. However, no individual filaments (body fossils), like they are typical for chert lithologies, can be recognized. The various microfacies morphologies can be grouped into five microfacies types. They are described in the following.

4.1.1. Microfacies (i)

Microfacies (i) displays a stack of fine laminae composed of organic matter (Fig. 3a). The thickness of such stacks ranges between 50 and 200 μm. The fine laminae are brown-opaque. Noteworthy, dark brown laminae alternate with light brown colored laminae. Thicknesses of individual dark and light brown laminae range from 5 to 15 μm. The laminae are not straight, but slightly irregular-wavy. Individual lenses of accumulated quartz grains may occur in between the laminae. Such lenses are between 70 and 100 μm wide and 10 to 30 μm high. The laminae around the lenses are bent. The edges of the stacks appear frayed, suggesting that they are large fragments of an originally laterally continuous layer.

4.1.2. Microfacies (ii)

Opaque, carbonaceous particles of round to oblong morphologies are typical for microfacies (ii), (Fig. 3c and d). In close-up view, the opaque particles appear undulose, meaning some areas are dark brown, whereas other areas appear lighter. Filamentous textures may surround individual particles, e.g. in Fig. 3d. Particle sizes range from 100 to 250 μm (longest diameter). The outline of the particles is irregular, showing very small embayments and lobes. Some particles appear more edgy than others. Fraying of edges, however, like in microfacies (i), does not occur.

Fig. 3. Biofilm microfacies in the Neoproterozoic Halkal Shale, Bhima basin, south India. (a, b) Biofilm microfacies (i) is a stack of carbonaceous laminae. Note the alternating dark and light laminae. (c) Biofilm microfacies (ii) are opaque particles with rounded edges; (d) the rounded particles show undulose opacity; (e) Biofilm microfacies (iii) is characterized by bifurcating and anastomosing laminae entangling a large amount of detrital grains (commonly quartz); (f) Close-up view of (e) showing net-work produced by brown opaque filamentous textures (a = slide no.-BSIP-16255; Q33; scale-200 μm; b = slide no.-BSIP-16255; S39; scale-200 μm; c = slide no.-BSIP-16252; T24; scale-100 μm; d = slide no.-BSIP-16252; Q33/4; scale-100 μm; e = slide no.-BSIP-16253; W28/7; scale-500 μm.

4.1.3. Microfacies (iii)

Microfacies (iii) is characterized by about 5 μm thin, opaque laminae that are arranged to a "loose" network (Fig. 3e and f). The material in between the laminae is light brown in color. The carbonaceous laminae are wavy-crinkly, with an orientation between horizontal and 40 degrees. Individual quartz grains occur. Mostly, they have no grain-to-grain contact. Such quartz grains may show a distinct orientation with their long-axes parallel to the bedding plane. In one thin-section, several quartz grains accumulated to a 100 μm long and 60 μm high lens.

4.1.4. Microfacies (iv)

The microfacies (iv) is characterized by elongated, opaque clasts that commonly are slightly folded, (Fig. 4 a). The opaque clasts show no "network"-like arrangement of laminae like microfacies (i) and (iii), but rather resemble the internal undulose make-up of microfacies (ii). Individual quartz grains occur. The long-axes of the grains do not show any preferred orientation.
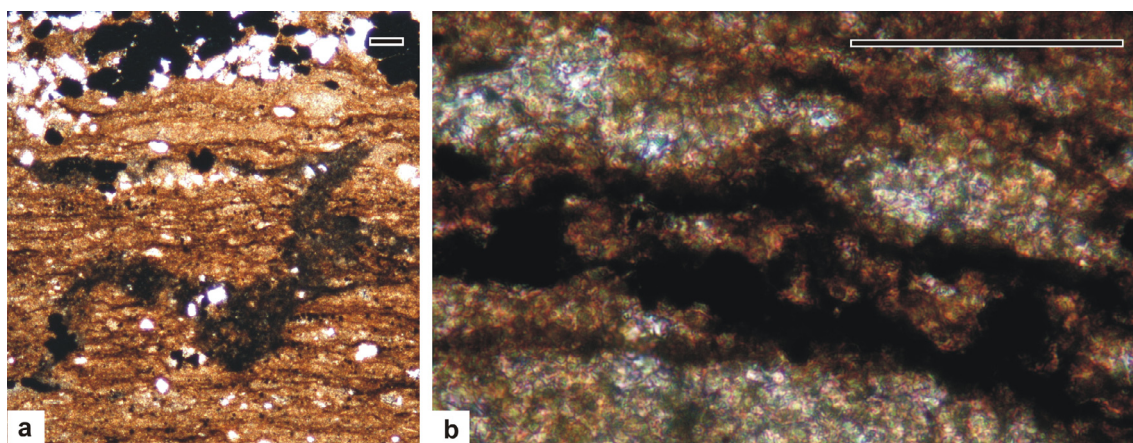
4.1.5. Microfacies (v)

In microfacies (v), individual bedding-parallel laminae that are located close to the rock bed surface may appear deformed. In close-up view, minerals such as pyrite and phosphorite are visible that may have deformed the laminae during crystal growth (Fig. 4b).

### 4.2. Raman spectroscopy of microfacies

Raman analyses of the putative fossil biofilms show that the microbial laminae are carbonaceous in nature (Fig. 5). Raman spectra of selected areas reveal the presence of two broad carbon peaks: D (Disordered peak) band and G (Graphite peak) band. The obtained spectra and the positions and widths of D and G peaks are characteristic of organic carbon (kerogen). Results on biofilm fragments also include the D-peak (Disordered peak) at 1338 cm^{-1} and G-peak (Graphite peak) at 1609 cm^{-1}. Incidentally both carbon and hematite have major peaks in the 1320–1350 cm^{-1} region, therefore the presence of organic carbon needs to be confirmed and mapped using the 1600 cm^{-1} peak (Marshall et al., 2011, Noffke et al., 2013). Raman analysis performed on the folded biofilm shows the absence of the D and G bands. The Raman spectra from the quartz-rich area lacks a carbon 1600 cm^{-1} peak. The carbonaceous laminae include fine grained pyrite and μm scale, elliptical nodules of phosphorous-rich apatite. Biotite flakes may line the carbonaceous layers, but are rarer compared to quartz grains. In the shale between the carbonaceous laminae, hematite and allochthonous quartz grains occur, as well as finely dispersed apatite.

4.3. X-ray-diffraction measurements on biofilms

X-ray diffraction studies of nodules and biofilms present in the bedded phosphorite revealed the mineral as flourapatite (Table 1, Fig. 6). It suggests that the Bhima phosphorite is sedimentary in nature. These are associated with major to minor quantities of quartz,

Fig. 4. Biofilm microfacies in the Neoproterozoic Halkal Shale, Bhima basin, south India. (a) Biofilm microfacies (iv) includes bent or rolled-up fragments of organic matter including some detrital grains; (b) Biofilm microfacies (v) are individual carbonaceous laminae of varying thicknesses due to intra-lamina pyrite crystal growth; (a = slide no.-BSIP-16253; L45; scale-100 μm; b = slide no.-BSIP-16252; C33/2; scale-100 μm).
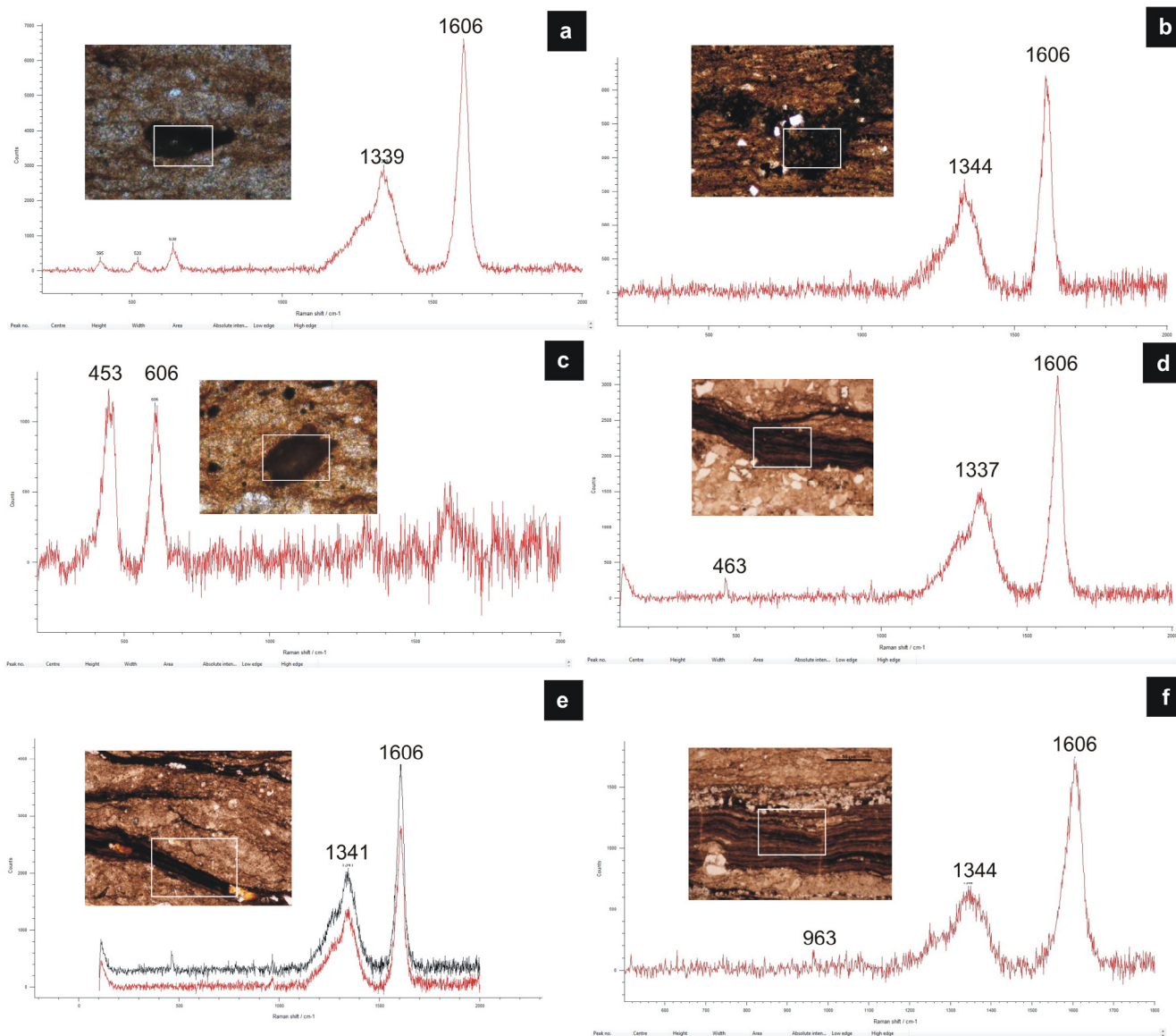
Fig. 5. Raman spectrographs of biofilm microfacies. The box in each photo shows the area of investigation. (a) Biofilm facies (ii) shows D-peak (Disordered peak) at 1341 cm^{-1} and G-peak (Graphite peak) at 1606 cm^{-1}; (b) Biofilm facies (iv) shows D-peak at 1339 cm^{-1} and G-peak at 1606 cm^{-1}; (c) Biofilm facies (ii) shows D-peak at 1338 cm^{-1} and G-peak at 1609 cm^{-1}. (d, e, f) show biofilm facies (i).

Table 1
Results of X-ray diffraction studies of phosphorite samples from the Halkal Formation, Bhima Basin.

Sample No.	Locality	Mineral phase	Gangue
BSIP-1	Upper band-1 Gangurthi	Flourapatite is main apatitic phase. Kaolinite and Muscovite are present in small proportions.	Quartz
BSIP-2	Upper band-2 Gangurthi	Flourapatite	Quartz
BSIP-3	Middle Band Gangurthi	Flourapatite	Quartz
BSIP-4	Lower Band Gangurthi	Flourapatite is main apatitic phase. Muscovite is also present	Quartz
BSIP-5	Pandurang temple (Ishwar temple)	Muscovite	Quartz
BSIP-6	Behind Primary School, Gangurthi	Flourapatite	Quartz

muscovite and kaolinite.

5. Discussion

Morphologically we interpret the microfacies as *in situ* fossilized biofilms. The biofilms probably developed in a shallow subtidal area close to the shoreline.

Microfacies (i) is here interpreted as fossil biolaminites. Such biolaminites are stacks of organic layers that each represents a generation of biofilm. The alternating pattern of dark and light brown laminae may be the result of seasonal growth, as it is known from cyanobacteria-dominated microbial mats in modern tidal and sabkha settings (Gerdes and Krumbein, 1987). Such biolaminites develop at sites of low net sedimentary input. This low sedimentation rate is reflected also in our samples by the comparably low amount of detrital quartz grains in the biolaminites. Low to moderate bottom currents may have provided sufficient nutrient supply, however did not exceed an erosional threshold that would have prohibited biofilm build-up. This biofilm facies resembles in morphology to the Klb laminations described from the ca. 3 Ga Buck Reef Chert, South Africa, where similar paleoconditions existed (Tice and Lowe, 2006).

Whereas microfacies (i) may record thicker biofilms that colonized sites of favourable growth conditions, microfacies (iii) may represent a less mature biofilm stage. The anastomosing and bifurcating morphologies of the laminae in microfacies (iii) resemble the Klm laminations in Tice and Lowe (2006), the carbonaceous shale in Schieber (1986, 1989), and the endobenthic microbial mat fabrics in Noffke (2010). All studies describe a relatively high amount of detrital grains in the microbial facies.

Some of the Buck Reef biofilms may have experienced episodic erosion during minor reworking events (Tice and Lowe, 2006). During such an event, the water motion ripped up the biofilm and redistributed the small fragments to other sites. Also, our microfacies (i) and (iv) may have been subjected to stronger bottom currents causing mechanical disruption and fragmentation of some of the organic layers. Subsequent transport by saltation and rolling transport across the sea floor may have formed the rounded particles of microfacies (ii). Their morphologies record an effective binding capacity of the ancient biofilms (Walsh and Lowe, 1999; Tice and Lowe, 2004, 2006).

Some of the biofilms may include a few detrital grains that appear to 'float' in the organic matrix. Whereas, silt-sized grains may have been derived by fall-out of suspension, sand-sized, 'floating' quartz grains may also represent particles from the substrate that were pulled upward during the growth of the biofilms. The orientation of the 'floating' grains with their long-axes parallel to the bedding suggests such an origin, because such grains dragged upward by biofilm tend to rotate during this transport (Noffke, 2010).

One open question about Neoproterozoic phosphorites is which group of microorganisms may have composed biofilms. Modern phosphorite formation can be observed on the westward shelves of Africa, the Americas, Australia and India in tropical up-welling zones (e.g., Crosby and Bailey, 2012). Williams and Reimers (1983) suggested that bacterial fossils in ancient phosphorites may represent chemosynthetic microorganisms that induced phosphogenesis. In their study, Hiatt et al. (2015) pointed out that "although the locus and scale of

phosphogenesis has changed, the fundamental relationship between chemosynthetic microbial communities and phosphate mineralization has existed over at least the last 1.85 Ga". Like in the modern, paleo-marine phosphatic units generally record time spans of mainly, but not exclusively, reducing benthic conditions leading to the precipitation of phosphorous in the context of biogenic matter (Sheldon, 1987; Burdige, 2006; Schiffbauer et al., 2014). Phosphogenesis in Neoproterozoic phosphorite in the stromatolitic peritidal limestones from Salitre Formation, Brazil, was restricted to the nearshore area (Caird et al., 2017). In this case, the phosphate was stored and concentrated in the interior of stromatolites by the activity of heterotrophic and chemosynthetic bacteria, which created the redox and sedimentological conditions for the authigenic precipitation of phosphorus. Criveling et al. (2014) discussed the source of phosphorous that occurs in phosphatic Cambrian carbonates from Australia. They suggest that organic decay and bacterial iron reduction were responsible for the enrichment of phosphates in those sediments, causing precipitation of apatite within small shelly fossils. In our example, one possible explanation for the precipitation of phosphates and consequent accumulation of phosphorites is the 'extracellular hypothesis' suggested by Caird et al. (2017). Here, bacteria create the redox condition for the accumulation of phosphate. In this case, the phosphate precipitation is a product of the bacterial metabolism in a phosphorous-rich medium. The own cell wall with their charge, or the extracellular polymeric substance (EPS) produced by bacteria may lead the mineral precipitation by providing nucleation sites and decreasing the activation energy for the reactions to occur (Ferris, 1989; Crosby and Bailey, 2012). The mechanism triggers when the oxygen is used as an electron acceptor on the external membrane of the sulfide-oxidizing bacterial cells, creating an acid medium, which favors phosphate precipitation. The hypothesis also can explain the presence of pyrite in the carbonaceous microfacies. The reducing environment created by the organic matter decay plus the sulfide-reducing bacterial activity (in contact with detrital iron minerals) can precipitate pyrite (FeS$_2$) (Berner, 1984, Canfield and Rainswell, 1991, Bird et al., 2001). By using the oxygen as electron acceptor, the sulfide-oxidizing bacteria can create an acid medium, which favors phosphate precipitation.

An alternative way is the 'intracellular hypothesis'. In our example, the accumulation of the phosphate mineral apatite as μm scale nodules in the carbonaceous laminae may point towards sulfide-oxidizing bacteria such as of the family Beggiatoaceae as biofilm-constituents. Under oxic conditions, these bacteria can accumulate intracellular polyphosphate as a mechanism of energy storage (Schulz and Schulz, 2005; Brock, 2011). In anoxic conditions, the microbes break the polyphosphate into phosphate, increasing the concentration of phosphate in the deposits. Indeed, Schulz and Schulz (2005) have observed phosphorous-rich pore waters in modern upwelling deposits overgrown by sulfide-oxidizing biofilms. Precursor, 'amorphous' precipitates crystallize into apatite over time (e.g., Schulz and Schulz, 2005; Goldhammer et al., 2010; Crosby and Bailey, 2012). The thickness of the phosphorite deposits in the Bhima Basin, and the large amount of accumulated minerals outsides the fossil biofilms may point toward an extracellular process. However, due to their small sizes, nodules constituted of phosphate mineral may point towards intracellular precipitation. The occurrence of both processes is possible.

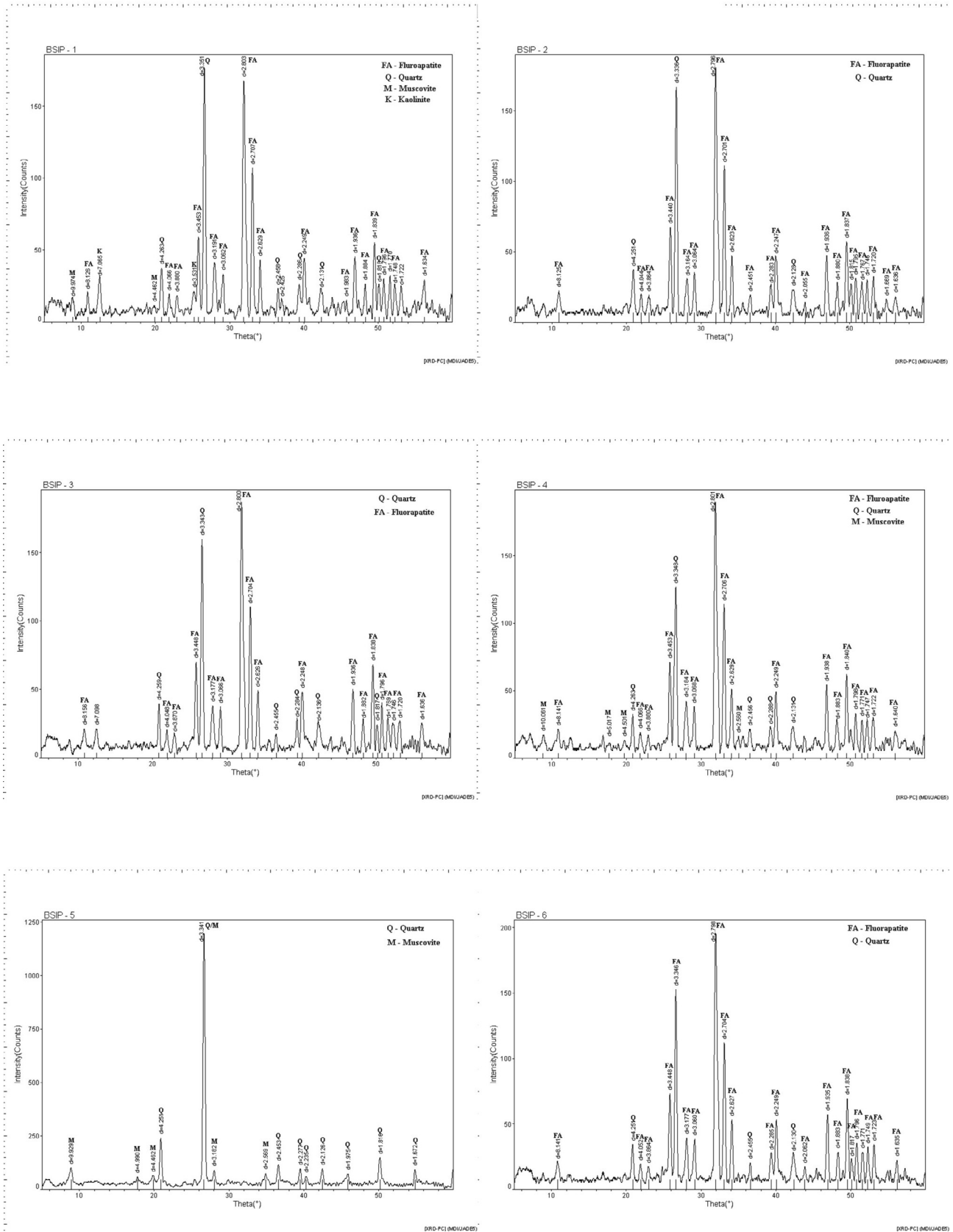## X-ray diffractograms of phosphorite samples

Fig. 6. Graphs obtained by the X-ray diffraction studies of phosphorite samples from the Halkal Shale, Bhima Basin, India.

The presence of pyrite in the biofilm facies is another indication for bio-precipitation. Ubiquitous sulfate reducing bacteria (SRB) co-occurring with sulfide oxidizing ones produce hydrogen sulfide that in presence of Fe contributes to subsequent pyrite formation (Joergensen, 1982). The microfacies (v) in the Halkal Shale units may represent microsites of increased Fe abundance.

Inorganic precipitation of phosphorite minerals in this extremely phosphorous-rich paleo-system is to be expected and may have been the cause for the finely dispersed apatite in the background sediments. Weathering plays an important role in concentration of phosphorite in carbonate-flourapatite rich zones. Low concentration of trace elements defines three major associations such as: apatitic phosphorites, ferruginous-clayey phosphorites and weathered (leached) aluminous phosphorites (Banerjee et al., 1982). It is established through trace element studies on the different phosphorite deposits of the world that the intensity of weathering depends on mineral association and a general tendency for the depletion of CO_2 in apatites leads to restrict the mineral transformation beyond fluorapatite stage (Lucas et al., 1980). The abundance of flourapatite in the Halkal Formation might be due to loss of CO_2 from carbonate-fluorapatite during repeated weathering, metamorphic and tectonic cycles experienced by the Proterozoic sedimentary succession besides weathering of rocks (Dayal et al., 1984). This depletion of CO_2 is an indicator of hidden weathering in the rocks (Banerjee et al., 1982). In modern marine upwelling zones, finely dispersed carbonate fluorapatite (CFA) is an abundant constituent in the sediments (Filippelli, 2011), and may significantly contribute to phosphorous enrichment in later consolidated phosphorites. Biotite flakes located alongside the carbonaceous laminae may have been trapped by the adhesive mucilage of the biofilm communities as soon as water motion allowed suspension to settle (see laboratory experiments on clay particle enrichment by Newman et al., 2016). They are simply allochthonous accumulations reflecting suspension and bed-load (back ground sediments) during calm hydrodynamic conditions. However, Ruttenberg and Berner (1993) described the dissolution of such Fe-bearing minerals under anoxic conditions. Fe-bearing minerals like biotite actually may absorb phosphorous in nutrient-rich water such as in upwelling zones. During their dissolution, the adsorbed phosphorous is released into the deposits (Crosby and Bailey, 2012).

In situ phosphatization of organic matter (e.g., Briggs et al., 1993) cannot be concluded from the fossil biofilm facies described here, because there is no direct association of textures with phosphorite. Due to lack of any recognizable body fossil, any assessment of the taxonomic group of the ancient microorganisms for this part of the Neoproterozoic world will remain speculative.

6. Conclusions

Fossil biofilms are reported from petrographic thin sections of the Neoproterozoic phosphorites of India. They form five distinct types of microfacies. The biofilms interacted with sedimentary processes in a shallow sub-tidal area. Small scaled roll-ups of biofilm demonstrate their effective binding capacity. In thin-section, the opaque brown laminae of the biofilms include homogeneous phosphate particles and organic matter (kerogen) of fossilized cell material and EPS. D and G bands of Raman analysis of the biofilms establish the organic nature of kerogen. The cell surface and the redox conditions created by the microbial metabolism in the immediate surrounding of the microbes induced extracellular mineral nucleation. The large amount and extension of the phosphates in Halkal Shale points to an extracellular precipitation by biologically-induced mineralization (when the cell surface and redox conditions created by the microbial metabolism induce the mineral nucleation and formation of mineral deposits). However, small size phosphate nodules inside the filaments may have been caused by intracellular processes. The absence of any recognizable body fossils (cells or filaments) does not allow conclusions on the taxonomic position of the microorganisms composing the biofilms.

References

Akhtar, K., 1977. Depositional environment, dispersal pattern and palaeogeography of the clastic sequence in the Bhima basin. Indian Mineral. 18, 65–72.

Arning, E.T., Birgel, D., Brunner, B., Peckmann, J., 2009. Bacterial formation of phosphatic laminites of Peru. Geobiology 7, 295–307.

Awramik, S.M., 1971. Precambrian columnar stromatolite diversity: Reflection of metazoan appearance. Science 174, 825–827.

Awramik, S.M., 1991. Archean and proterozoic stromatolites. In: Riding, R. (Ed.), Calcareous Algae and Stromatolites. Spring-Verlag, Berlin, pp. 289–304.

Banerjee, D.M., 1971a. Aravallian stromatolites from Udaipur, Rajasthan, India. J. Geol. Soc. India 12 (4), 349–355.

Banerjee, D.M., 1971b. Precambrian Stromatolitic phosphorites of Udaipur, Rajasthan, India. Geol. Soc. Am. Bull. 82 (8), 2319–2330.

Banerjee, D.M., Khan, M.W.Y., Srivastava, N., Saigal, G.C., 1982. Precambrian phosphorites in the Bijawar Rocks of Hirapur-Bassia area, Sagar District, Madhya Pradesh, India. Miner. Deposita 17, 349–362.

Berner, R.A., 1984. Sedimentary pyrite formation: an update. Geochim. Cosmochim. Acta 48, 605–615.

Bird, D.F., Juniper, S.K., Ricciardi-Rigault, M., Martineu, P., Prairie, Y.T., Calvert, S.E., 2001. Subsurface viruses and bacteria in Holocene/Late Pleistocene sediments of Saanich Inlet, B.C.: ODP Holes 1033B and 1034B, Legs 169S. Mar. Geol. 174, 227–239.

Bower, D.M., Steele, A., Fries, M.D., Green, O.R., Lindsay, J.F., 2016. Raman imaging spectroscopy of a putative microfossil from the 3.46 Ga Apex Chert: Insights from Quartz Grain Orientation. Astrobiology 16 (2), 169–180.

Briggs, D., Kear, A.J., Martill, D.M., Wilby, T.R., 1993. Phosphatization of soft tissue in experiments and fossils. J. Geol. Soc. Lond. 150, 1035–1038.

Brock, J., 2011. Impact of Sulfide-Oxidizing Bacteria on The Phosphorous Cycle In Marine Sediments (PhD-thesis). University of Bremen, pp. 93.

Burdige, D.J., 2006. Geochemistry of Marine Sediments. Princeton University Press, pp. 609.

Caird, R.A., Pufahl, P.K., Hiatt, E.E., Abram, M.B., Dourado, A.R., Kyser, T.K., 2017. Ediacaran stromatolites and intertidal phosphorite of the Salitre Formation, Brazil: Phosphogenesis during the Neoproterozoic Oxygenation Event. Sed. Geol. 350, 55–71.

Canfield, D.E., Poulton, S.W., Narbonne, G.M., 2007. Late-Neoproterozoic deep-ocean oxygenation and the rise of animal life. Science 315, 92–95.

Canfield, D.E., Rainswell, R., 1991. Pyrite formation and fossil preservation. In: Alisson, P.A., Briggs, D.E.G. (Eds.), Taphonomy: Releasing The Data Locked In The Fossil Record. Plenum Press, New York, pp. 337–387.

Chalapathi Rao, N.V., Anand, M., Dongre, A., Osborne, I., 2010. Caerbonate xenoliths hosted by the Mesoproterozoic Siddanpalli Kimberlite cluster (Eastern Dharwar Craton): implications for the geodynamic evolution of southern India and its diamond and uranium metallogenesis. Int. J. Earth Sci. 99, 1791–1804.

Criveling, J.R., Johnston, D.T., Poulton, S.W., Kotrc, B., März, C., Schrag, D.P., Knoll, A.H., 2014. Phosphorus sources for phosphatic Cambrian carbonates. Geol. Soc. Am. Bull. 126, 145–163.

Crosby, C.H., Bailey, J.V., 2012. The role of microbes in the formation of modern and ancient phosphatic minerals deposits. Front. Microbiol. 3, 1–7.

Crosby, C.H., Bailey, J., Sharma, M., 2014. Fossil evidence of ironoxidizing chemolithotrophy linked to phosphogenesis in the wake of the Great Oxidation Event. Geology 42, 1015–1018.

Das Sarma, D.C., Raha, P.K., Moitra, A.K., Ashok Kumar, P., Anantharaman, S., Rama Rao, U., Sundaram, V., 1992. Discovery of Precambrian-Cambrian transitional fossil Sabellitids from India. Curr. Sci. 63, 140–142.

Dayal, B., Jamwal, R.S., Negi, R.S., Sinha, A.P., Chaurasia, P.K., Hore, M.K., 1984. Phosphorite occurrences in Delhi Supergroup, Northeastern Rajasthan. Phohosphorite. Geol. Surv. India Spec. Publ. 17, 129–133.

Dongre, A., Chalapathi Rao, N.V., Kamde, G., 2008. Limestone xenolith in Siddanpalli Kimberlite, Gadwal Granite-Greenstone Terrain, Eastern Dharwar Craton, Southern India: Remnant of Proterozoic Platformal cover sequence of Bhima/Kurnool age? J. Geol. 116, 184–191.

Dornbos, S.Q., Bottjer, D.J., Chen, J.Y., 2004. Evidence for seafloor microbial mats and associated metazoan lifestyle in Lower Cambrian phosphorites of Sothwest China. Lethaia 37, 127–137.

Dzik, J., 2007. The Verdun Syndrome: simultaneous origin of protective armour and in-faunal shelters at the Precambrian–Cambrian transition. In: Vickersrich, P., Komarower, P. (Eds.), The Rise and Fall of the Ediacaran Biota. Geological Society, Special Publications, London, pp. 405–414.

Fedonkin, M.A., 2003. The origin of Metazoa in the light of Proterozoic fossil record. Paleontolog. Res. 7, 9–41.

Ferris, F.G., 1989. Metallic ion interactions with the outer membrane of gram-negative bacteria. Wiley, New York, pp. 295–323.

Filippelli, G.M., 2011. Phosphate rock formation and marine phosphorous geochemistry: the deep time perspective. Chemosphere 84, 759–766.

Filippelli, G.M., Delaney, M.L., 1994. The oceanic P cycle and continental weathering during the Neogene. Paleoceanography 9, 643–652.

Foote, R.B., 1876. The geological features of the South Mahratta country and adjoining districts. Memoir. Geol. Survey India 12, 70–138.

Gamper, A., Heubeck, C. and Demske, D., 2012. Composition and microfacies of Archean microbial mats (Moodies Group, ca. 3.22 Ga, South Africa).- in: Microbial Mats in Siliciclastic Depositional Systems Through Time, eds. Noffke, N. and Chafetz, H., SEPM Special Publication No. 101, SEPM (Society for Sedimentary Geology), pp. 65–74.

Gerdes, G., Krumbein, W.E., 1987. Biolaminated Deposits. Lecture Notes in Earcth Sciences. Springer-Verlag, New York, pp. 183.

Goldhammer, T., Bruechert, V., Ferdelman, T.G., Zabel, M., 2010. Microbial sequestration of phosphorous in anoxic upwelling sediments. Nat. Geosci. 3, 557–561.

Hiatt, E.E., Pufahl, P.K., Edwards, C.T., 2015. Sedimentary phosphates and associated fossil bacteria in Paleoproterozoic tidal flat in the 1.85 Ga Michigamme Formation, Michigan, USA. Sed. Geol. 310, 24–39.

Heubeck, C., 2009. An early ecosystem of Archean tidal microbial mats (Moodies Group, South Africa, ca. 3.2 Ga). Geology 37 (10), 931–934.

Janardhan Rao, L.H., Srinivas Rao, C., Ramakrishna, T.L., 1975. Re-classification of the rocks of Bhima basin, Gulbarga district, Mysore state. Geol. Surv. India Miscell. Publ. 23, 177–184.

Jayaprakash, A.V., 2007. Purana Basins of Karnataka. Memoirs Geol. Surv. India 129, 87–136.

Joergensen, B.B., 1982. Mineralization of organic matter in the seabed – the role of sulfate reduction. Nature 296, 693–1649.

Kale, V.S., Peshwa, V.V., 1995. Bhima Basin. In: Field Guide Book. Geological Society of India, Bangalore, pp. 142.

Kale, V.S., Mudholkar, A.V., Phansalkar, V.G., Peshwa, V.V., 1990. Stratigraphy of the Bhima Group. J. Palaeontol. Soc. India 35, 91–103.

Kumar, B., Das, S., Shukla, M., Sharma, M., 1999. Chronostratigraphic implication of Carbon and Oxygen isotopic compositions of the Proterozoic Bhima carbonates, Southern India. J. Geol. Soc. India 53, 593–600.

Lamboy, M., 1994. Nannostructure and genesis of phosphorites from ODP Leg 112, the Peru margin. Mar. Geol. 118, 5–22.

Lepland, A., Joosu, L., Kirsimae, K., Prave, A.R., Romashkin, A.E., Crne, A.E., Martin, A.P., Fallick, A.E., Somelar, P., Upraus, K., Mand, K., Roberts, N.M.W., vanZuilen, M.A., Wirth, R., Schreibe, A., 2013. Potential influence of sulphur bacteria on Palaeoproterozoic phosphogenesis. Nat. Geosci. 7, 20–24.

Lucas, J., Flicoteaux, R., Nathan, Y., Pretov, L., Shahar, Y., 1980. Different aspects of Phosphorite weathering. SEPM Special Publication No. 29, 41–51.

Mahadevan, C., 1947. The Bhima Series and other rocks in Gulbarga district. J. Hyderabad Geol. Survey 5, 1–82.

Maithy, P.K., Babu, R., 1996. Carbonaceous macrofossils and organic-walled microfossils from the Hulkal Formation, Bhima Group, Karnataka with remark on age. Palaeobotanist 45, 1–6.

Marshall, C.P., Emry, J.R., Marshall, A.O., 2011. Haematite pseudomicrofossils present in the 3.5-billion-year-old Apex Chert. Nat. Geosci. 4, 240–243.

Malur, M.N., Nagendra, R., 1994. Lithostratigraphy of the Bhima basin (central part), Karnataka, Southern India. J. Palaeontol. Soc. India 39, 55–60.

Mathur, S.M., 1977. Some aspects of the stratigraphy and limestone resources of the Bhima Group. Indian Mineral. 18, 59–64.

Mathur, S.M., 1979. A note on Glauconite in the Bhima Group. Indian Minerals 31 (4), 57–58.

Mishra, R.N., Jayaprakash, A.V., Hans, S.K., Sundram, V., 1987. Bhima Group of Proterozoic-a stratigraphic puzzle. Memoir Geol. Soc. India 6, 227–237.

Mudholkar, A.V., Kale, V.S., 1982. Lithostratigraphy of the Rabanpalli Shale Formation, Bhima Group, Rabanpalli area, Karnataka. In: Proceedings 10th Indian Colloquium Micropalaeontology and Stratigraphy, pp. 97–110.

Nathan, Y., Bremner, J.M., Lowenthal, R.E., Monteiro, P., 1993. Role of bacteria in phosphorite genesis. Geomicrobiol. J. 11, 69–76.

Nelson, J.G., Pufahl, P.K., Hiatt, E.E., 2010. Paleoceanographic constraints on Precambrian phosphorite accumulation, Baraga Group, Michigan, USA. Sediment. Geol. 226, 9–21.

Newman, S.A., Klepac-Ceraj, V., Mariotti, G., Pruss, S., Watson, N., Bosak, T., 2016. Experimental fossilization of mat-forming cyanobacteria in coarse-grained silici-clastic sediments. Geobiology 15, 484–498.

Noffke, N., 2000. Extensive microbial mats and their influences on the erosional and depositional dynamics of a siliciclastic cold-water environment (Lower Arenigian, Montagne Noire, France). Sed. Geol. 136, 207–215.

Noffke, N., 2010. Microbial Mats in Sandy Deposits From the Archean To Today. Springer, New York, pp. 196.

Noffke, N., Christian, D., Wacey, D., Hazen, R.M., 2013. Microbially Induced Sedimentary Structures recording an ancient ecosystem in the ca. 3.48 Billion-Year-Old Dresser Formation, Pilbara, Western Australia. Astrobiology 13 (12), 1103–1124.

Och, L.M., Shields-Zhou, G., 2012. The Neoproterozoic oxygenation event: Environmental perturbations and biogeochemical cycling. Earth Sci. Rev. 110, 26–57.

Pandey, B.K., Natarajan, V., Veena Krishna and Pandit, S.A., 2008. U–Pb and Sm–Nd isotopic studies on uraniferous brecciated limestone from Bhima basin: evidence for a Mesoproterozoic mineralization event in southern peninsular India, In: Significant milestones in the growth of geochemistry in India during the 50 years period: 1958–2008. Jointly organized by Geological Society of India and AMD, Hyderabad, (Abs). pp. 24–25.

Papineau, D., 2010. Global biogeochemical changes at both ends of the Proterozoic: in-sights from phosphorites. Astrobiology 10, 165–181.

Papineau, D., Purohit, R., Fogel, M.L., Shields-Zhou, G.A., 2013. High phosphate avail-ability as a possible cause for massive cyanobacterial production of oxygen in the Paleoproterozoic atmosphere. Earth Planet. Sci. Lett. 362, 225–236.

Pufahl, P.K., 2010. Bioelemental sediments. In: James, N.P., Dalrymple, R.W. (Eds.), Facies Models, 4th ed. Geological Association of Canada, pp. 477–503.

Riding, R., 2006. Microbial carbonate abundance compared with fluctuations in me-tazoan diversity over geological time. Sed. Geol. 185, 229–238.

Ruttenberg, K.C., Berner, R.A., 1993. Authigenic apatite formation and burial in sedi-ments from non-upwelling continental margin environments. Geochim. Cosmochim. Acta 59, 991–1007.

Salujha, S.K., Rehman, K., Arora, C.M., 1970. (published 1972). Microplankton from the Bhima. J. Palaeontol. Soc. India 15, 10–16.

Sallstedt, T., Bengtson, S., Broman, C., Crill, P.M., Canfield, D.E., 2017. Evidence of oxygenic phototrophy in ancient phosphatic stromatolites from the Paleoproterozoic Vindhyan and Aravalli Supergroups, India. Geobiology 16, 139–159.

Sathyanarayan, S., Arneth, J.D., Schidlowski, M., 1987. Stable Isotope Geochemistry of Sedimentary Carbonates from the Proterozoic Kaladgi, Badami and Bhima Groups, Karnataka, India. Precambr. Res. 37, 147–156.

Schieber, J., 1986. The possible role of benthic microbial mats during the formation of carbonaceous shales in shallow Mid-Proterozoic basins. Sedimentology 33, 521–536.

Schieber, J., 1989. Pyrite mineralization in microbial mats from the mid-Proterozoic Newland Formation, Belt Supergroup, Montana, U.S.A. Sed. Geol. 64, 79–90.

Seilacher,, 1999. A. Biomat-related lifestyles in the Precambrian. Palaios 14, 86–93.

Sharma, M. and Shukla, M., 1996. Diversity and gigantism of carbonaceous macrofossils in Terminal Proterozoic Bhima basin of India: Abstracts 30th International Geological Congress, Beijing, China, 2, 52.

Sharma, M., Shukla, Y., 2012. Megascopic carbonaceous compression fossils from Neoproterozoic Bhima Basin, Karnataka, South India. Geol. Soc. Lond. Spec. Publ. 366, 277–293.

Schulz, H.N., Schulz, H.D., 2005. Large sulfur bacteria and the formation of phosphorite. Science 307, 416–418.

Schiffbauer, J.D., Xiao, S., Cai, Y., Wallace, A.F., Hua, H., Hunter, J., Xu, H., Peng, Kaufman, A.J., 2014. A unifying model for Neoproterozoic-Palaeozoic exceptional fossil preservation through pyritization and carbonaceous compression. Nat. Commun. 5, 5754.

She, Z., Strother, P., McMahon, G., Nittler, L.R., Wang, J., Zhang, J., Sang, L., Ma, C., Papineau, D., 2013. Terminal Proterozoic cyanobacterial blooms and phosphogenesis documented by the Doushantuo granular phosphorites I: In situ micro-analysis of textures and composition. Precambr. Res. 235, 20–35.

Sheldon, P.R., 1987. Association of phosphorites, organic-rich shales, chert and carbonate rocks: Evaporites and. Carbonates 2, 7.

Shukla, Y., 2011. Palaeobiology of Terminal Proterozoic Bhima Basin, Karnataka. University of Lucknow, India (Unpublished Thesis).

Srinivasa, T.N., Sambe Gowda, S., 1970. Fossil Acritarcha from the Bhima "Series" of the Gulbarga district Mysore State, and their geological significance. In: Lakhsmann, S., West, W.D. (Eds.), Proceedings of the Symposium on the Purana Formation of Peninsular India, pp. 149–159.

Sood, N.K., Syamal Rao, S., 1984. Phosphorite in Bhima Basin, Southern Regional News. Geol. Surv. India 3, 13.

Soudry, D., Champetier, Y., 1983. Microbial processes in the Negev phosphorites (southern Israel). Sedimentology 30, 411–423.

Sun, Weiguo and Sharma, M., 2016. Ediacaran Body fossils and trace fossils from the Hotpet Sandstone of the Bhima Group in the Bhima Basin, southern India. Abstract 117, Geological Society of Australia Editors Laurie, J. R., Kruse, P. D., Gracia-Bellido, D. C. and Holmes, J. D., p. 57.

Suresh, R., Sundara Raju, T.P., 1983. Problematic *Chuaria* from the Bhima Basin, south India. Precambr. Res. 23, 79–85.

Tice, M.M., 2009. Environmental controls on photosynthetic microbial mat distribution and morphogenesis on a 3.42 Ga clastic-starved platform. Astrobiology 9, 989–1000.

Tice, M., Lowe, D.R., 2004. Photosynthetic microbial mats in the 3,4316 Myr old ocean. Nature 431, 549–552.

Tice, M., Lowe, D.R., 2006. The origin of carbonaceous matter in pre-3.0 Ga greenstone terrains: a review and new evidence from the 3.42 Ga Buck Reef Chert. Earth Sci. Rev. 76, 259–300.

Venkatachala, B.S., Rawat, M.S., 1973. Organic remains from the Bhima basin and re-marks on the age of Vindhyans and subsurface sediments in the Ganga valley. Geophytology 2, 107–117.

Viswanathiah, M.N., Venkatachalapathy, V., Doddiah, D., 1976. Palynofossils from Bhimas, Karnataka, South India. In: Proceedings of the 6th Indian Colloquium on Micropalaeontology and Stratigraphy, pp. 384–389.

Walsh, M.M. and Lowe, D.R. 1999. Modes of accumulation of carbonaceous matter in the

early Archean: a petrographic and geochemical study of the carbonaceous cherts of the Swaziland Supergroup. In: Lowe, D.R., Byerly, G.R. (Eds.), Geologic Evolution of the Barberton Greenstone Belt, South Africa: Geological Society of America Special Paper, 329: 115–132.

Westall, F., Folk, R.L., 2003. Exogenous carbonaceous microstructures in Early Archaean cherts and BIFs from the Isua Greenstone Belt: implications for the search for life in ancient rocks. Precambr. Res. 126 (3–4), 313–330.

Williams, L.A., Reimers, C.E., 1983. The role of bacterial mats in oxygen deficient marine basins and coastal upwelling regimes: A preliminary report. Geology 11, 267–269.